Basic building units and properties of a fluorescence single plane illumination microscope

K. Greger,[a),b)] J. Swoger,[c)] and E. H. K. Stelzer[a),d)]
Light Microscopy Group, Cell Biology and Biophysics Unit, EMBL-Heidelberg, Meyerhofstrasse 1, D-69117 Heidelberg, Germany

(Received 6 November 2006; accepted 30 November 2006; published online 28 February 2007)

The critical issue of all fluorescence microscopes is the efficient use of the fluorophores, i.e., to detect as many photons from the excited fluorophores as possible, as well as to excite only the fluorophores that are in focus. This issue is addressed in EMBL's implementation of a light sheet based microscope [single plane illumination microscope (SPIM)], which illuminates only the fluorophores in the focal plane of the detection objective lens. The light sheet is a beam that is collimated in one and focused in the other direction. Since no fluorophores are excited outside the detectors' focal plane, the method also provides intrinsic optical sectioning. The total number of observable time points can be improved by several orders of magnitude when compared to a confocal fluorescence microscope. The actual improvement factor depends on the number of planes acquired and required to achieve a certain signal to noise ratio. A SPIM consists of five basic units, which address (1) light detection, (2) illumination of the specimen, (3) generation of an appropriate beam of light, (4) translation and rotation of the specimen, and finally (5) control of different mechanical and electronic parts, data collection, and postprocessing of the data. We first describe the basic building units of EMBL's SPIM and its most relevant properties. We then cover the basic principles underlying this instrument and its unique properties such as the efficient usage of the fluorophores, the reduced photo toxic effects, the true optical sectioning capability, and the excellent axial resolution. We also discuss how an isotropic resolution can be achieved. The optical setup, the control hardware, and the control scheme are explained in detail. We also describe some less obvious refinements of the basic setup that result in an improved performance. The properties of the instrument are demonstrated by images of biological samples that were imaged with one of EMBL's SPIMs. © *2007 American Institute of Physics.* [DOI: 10.1063/1.2428277]

I. INTRODUCTION

Fluorescence microscopy is a widely used technique in the modern life sciences. The discovery of green fluorescent protein (GFP) and the development of tools to fuse them to proteins of interest have been of major importance. Expressing GFP-labeled proteins in living organisms is now a widely used method to investigate processes in molecular biology.[1,2] In combination with other techniques, such as immunolabeling and fluorescence tagging, many biological processes can now be observed in excellent detail.

Modern fluorescence microscopy measures the spatiotemporal, three-dimensional (3D) distribution of one or more fluorophores, and thus indirectly the distributions of proteins, lipids, and other molecules. Different microscopy techniques can be used, from simple wide-field fluorescence microscopy, which gives very little information about the third dimension, to more sophisticated methods such as confocal or multiphoton microscopies or single plane illumination microscopy (SPIM),[3–5] which provide information along the third dimension.

Confocal fluorescence microscopy is currently the most widely used technique to obtain three-dimensional data sets.[6] In these instruments the illumination and detection axes overlap in an antiparallel manner (commonly known as an epifluorescence arrangement). The use of a single lens with a limited numerical aperture results in an anisotropic point spread function (PSF), which is elongated along the z axis. The confocal theta microscope, a predecessor of the SPIM, addressed the anisotropic resolution by orthogonal confocal point-by-point illumination and detection. With this setup the resulting PSF is nearly isotropic.[7–9]

The SPIM is the wide-field version of the confocal theta microscope. The entire focal plane of the detection lens is illuminated from the side (Fig. 1). An entire plane is imaged in parallel, although at the expense of isotropy and lateral resolution when compared to confocal theta fluorescence microscopy. However, especially in low numerical aperture (NA) systems, the axial resolution is considerably better than in standard confocal setups.[10] The SPIM should be regarded as a combination of an independently operated illumination and a detection system (Fig. 2). Each can work with relatively low numerical apertures, but in combination they form

[a)]Authors to whom correspondence should be addressed.
[b)]Electronic mail: greger@embl.de
[c)]Present address: Systems Biology Programme, Center for Genomic Regulation, Passeig Marítim 37-49, 08003 Barcelona, Spain.
[d)]Electronic mail: stelzer@embl.de

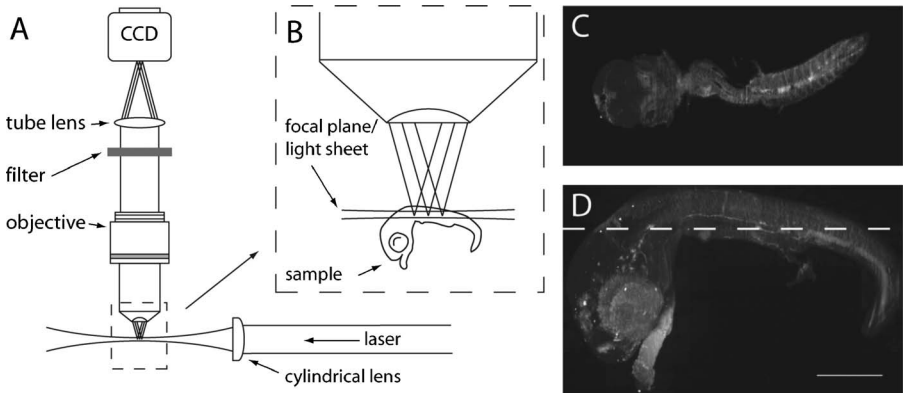

FIG. 1. The SPIM principle. (A) The central element of a SPIM is an essentially regular fluorescence microscope. It consists of an objective lens, a filter, a tube lens, and a wide-field detector. In contrast to the epifluorescence arrangement of conventional wide-field and confocal microscopes, no dichroic beam splitter is required to separate the illumination and detection light. Instead, the specimen is illuminated from the side by focusing a collimated laser beam to a light sheet with a cylindrical lens. Hence, only a thin volume around the geometric focal plane of the objective lens is illuminated. (B) In the specimen, only those fluorophores that are actually observed are also illuminated. This leads to optical sectioning and does not generate photodamage outside the focal plane. (C) A single image out of a stack of 500 planes, which was recorded about 200 μm inside a fixed PAX6 *in situ* medaka embryo (Ref. 17), demonstrates the optical sectioning capability, the excellent signal to noise ratio, and the extremely low background. (D) Sagittal projection of the stack of 500 images recorded at different depths. The dashed line indicates the plane in which the image shown in C was recorded. Recording conditions: λ_{ill}=488 nm, detection filter Chroma HQ 525/50 nm, detection lens Carl Zeiss Fluar 5×/0.25, scale bar 0.3 mm, recording time 200 ms/image, image size 1570×950 μm^2, 1217 pixel×736 pixel. Sample prepared by Mirana Ramialison.

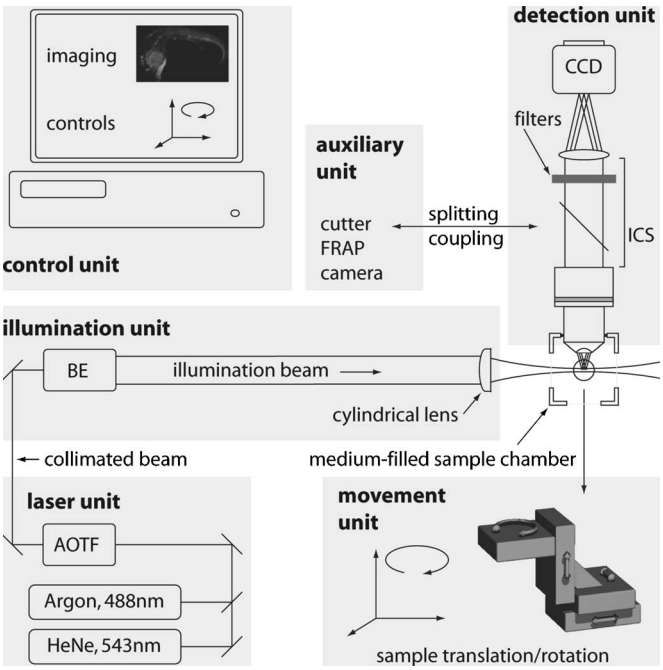

FIG. 2. The building units of a SPIM. The *detection unit* is a simplified fluorescence wide-field microscope. An objective lens, a filter, and a tube lens form the fluorescence image on the wide-field detector (CCD). The sample can be immersed in a medium-filled chamber for optimal experimental conditions. The *illumination unit* generates the light sheet for the illumination of the focal plane in the sample. A beam expander (BE) adjusts the diameter of a collimated beam and feeds it into a cylindrical lens. The *laser unit* delivers a collimated beam to the illumination unit. An acousto-optic tunable filter (AOTF) picks at least one of the several laser wavelengths and adjusts its intensity. The *movement unit* holds the sample and moves it relative to the optical setup. Three translational and one rotational stages allow positioning and scanning of the sample. Finally, the *control unit*, a standard computer equipped with data acquisition boards, controls the hardware and acquires the data. Additional optical elements such as beam couplers and splitters for *auxiliary units* can be introduced in the infinity corrected space (ICS) between the objective lens and the tube lens and will require further lasers and other optical components not shown here.

a PSF whose axial extent is smaller than in a conventional or a mid- to low-NA confocal fluorescence microscope, and therefore results in superior imaging properties. Such properties of the SPIM are of particular interest when imaging large intact samples, such as drosophila or fish embryos or united cell structures like Madin-Darby canine kidney (MDCK) cysts, *in vivo*.[11]

Another advantage of SPIM is its efficient use of the fluorophores, since only those in the focal plane are illuminated. During the acquisition of a stack of images, each plane is illuminated just once. The fluorophores outside the focal plane of the detection system are not illuminated and therefore not subject to photodamage. Compared to confocal and conventional microscopy, the fluorophores are used in a very efficient way and photodamage (e.g., bleaching) is greatly reduced. In confocal and conventional fluorescence microscopy the whole sample is illuminated while imaging every single plane, but only the information in the focal plane is used. This results in a much higher exposure (essentially by a factor determined by the number of the acquired planes). In SPIM phototoxic effects are also greatly reduced compared to other techniques.

An additional feature of EMBL's SPIM is that the sample can be rotated and three-dimensional stacks of images can be acquired along multiple directions. These stacks can be fused to combine the information into a single three-dimensional stack.[12] This procedure has two advantages. First, the extent of the PSF of the combined data sets is dominated by the highest resolution, which is in general provided along the lateral axes. The axial extent of the multiview PSF becomes identical to the lateral extents. Thus the volume resolution becomes considerably better and isotropic. Second, information hidden behind opaque structures in the sample along one view can be complemented by the information obtained along another view. Therefore, the multiview SPIM can determine the three-dimensional fluorophore distribution of relatively large samples. The low background

TABLE I. The basic building units of the SPIM setup.

Unit	Purpose	Main elements
Detection	Image formation	CCD, tube lens, filter, and objective lens
Illumination	Creating the light sheet	Beam expander and cylindrical lens
Laser	Providing the right wavelength and intensity	Lasers and AOTF
Movement and sample holder	Holding and manipulating the sample	Translation and rotation stages
Control	Control and timing of the elements	Computer, stage controller, and software
Auxiliary	Providing additional functionality (cutter, patterned photobleaching, FLIM, etc.)	Scan mirrors and UV laser

and the high signal to noise ratio (mainly due to the parallel recording with a camera) of SPIM data are prerequisites for effective data processing. The details of the image processing procedure involved will be the subject of a future work.

II. SETUP

A SPIM consists of five basic units. The *detection unit* is a simplified fluorescence wide-field (i.e., digital camera based) microscope. The *illumination unit* forms the light sheet, which illuminates the small portion of the sample that is found in the focal plane of the detection unit. The *laser unit* provides collimated beams from several light sources for the illumination unit. The *movement unit* holds the sample and moves it relative to the stationary optical setup. Finally, the *control unit* operates the hardware and controls the data acquisition process. Auxiliary additions (see Fig. 2 and Table I) provide manipulation tools such as a laser cutter or a scanner for patterned photobleaching.

The optomechanical parts are mounted on a 65 mm rail system (SYS 65, OWIS GmbH, Germany). The detection system is enclosed in a custom-made housing to block ambient and stray excitation light. The whole system is controlled by a program written in LABVIEW 7.1 (National Instruments). Once the data are acquired, the data sets are transferred to another computer, which performs further data processing.

A. Detection unit

The detection unit is similar to that of a conventional fluorescence microscope. It consists of an objective lens, a filter wheel, a tube lens, and a wide-field detector (e.g., a camera). Since we deal with biological samples, we rely mainly on water dipping lenses (Carl Zeiss AG, Germany, Achroplan $10\times/0.3$ W, Achroplan $20\times/0.5$ W, Achroplan $40\times/0.8$ W, Achroplan $63\times/0.9$ W, and Achroplan $100\times/1.0$ W) but we also use standard air lenses (Carl Zeiss AG, Germany, Fluar $5\times/0.25$ and Epiplan $10\times/0.2$) for lower magnifications. An emission filter blocks the excitation light and transmits the fluorescence signal emitted by the sample. Chroma filters of the HQ series or RazorEdge filters from Semrock (Rochester, NY) have performed very well until now. For the fluorescent proteins GFP a 500 nm long pass filter (emHQ500LP, Chroma Technology Corp., Rockingham, NC) or a RazorEdge LP01-488RU-25 (Semrock, Rochester, NY) is used. A 50 nm bandpass around 525 nm (emHQ525BP50, Chroma Technology Corp., Rockingham, NC) is used, if autofluorescence has to be suppressed. The filters are mounted in a computer-controlled filter wheel (Lambda 10-3, Sutter Instrument, CA). The tube lens (45 29 60, Zeiss, Germany) forms the primary image on the charge coupled device (CCD) chip of a camera [Hamamatsu ORCA, C4742-80-12AG, resolution: 1344×1024, pixel pitch: 6.45 μm, frame rate: up to 8 fps (fps denotes frame per second) in full frame and up to 41 fps with 8×8 binning, Hamamatsu Photonics K.K., Japan]. Extra beam splitters/couplers and filters can be introduced into the infinitely corrected space (ICS) between the objective and the tube lens but are not required in the standard setup.

B. Illumination unit

The illumination unit uses a collimated beam of light and generates a light sheet (Fig. 3). The collimated beam is expanded to the required diameter for a given sample by a zoom beam expander ($1\times-8\times$, S6ASS2075-067, Sill Optics GmbH, Germany).

The simplest setup would use a single cylindrical lens located at its focal distance from the detection axis. However, cylindrical lenses with the required NA are not easily available as well-corrected elements and tend to introduce unacceptable aberrations. Therefore, an objective lens (e.g., an Epiplan $10\times/0.2$, Carl Zeiss AG, Germany) is used in combination with a cylindrical lens that is rotated by 90°. The objective and the cylindrical singlet lenses form a telescope along the direction parallel to the focal plane of the detection system. The focal plane of the objective is on the axis of the detection system, and the focal plane of the cylindrical lens is in the back focal plane of the objective. Along the dimension perpendicular to the light sheet plane, the cylindrical lens does not refract the beam. With this arrangement, diffraction limited light sheets can be obtained.

With the setup it is also possible to exactly superimpose the light sheet on the focal plane of the detection system. The plane on which the detection system focuses is optimally illuminated. The two lenses L1 and L2 [Fig. 3(c)] form a telescope. The back focal plane of the illumination objective and the mirror in the gimbal mount (26.306.038, OWIS GmbH, Germany) lie in conjugated planes. When the beam is tilted around the center of the conjugated plane, the light sheet is moved along the optical axis of the detection system without being tilted.

C. Laser unit

The laser unit combines the beams from several lasers and provides a centered collimated beam for the illumination unit. Three different lasers are used as light sources. An argon laser provides lines at 488 and 514 nm (35 LAL 030-230, Melles Griot, CA) and two HeNe lasers operate at 543 nm (25-LGP-193-230, Melles Griot, CA) and 633 nm (25 LHR 991-230, Melles Griot, CA). The laser beams are

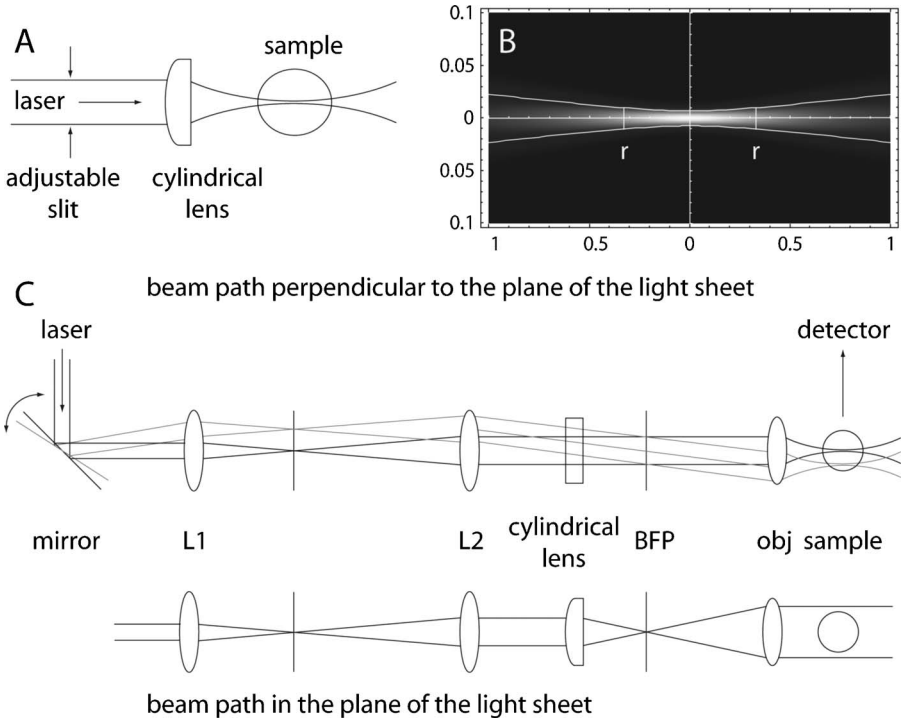

FIG. 3. Optical layout of illumination unit. (A) The most basic setup to create a light sheet uses a single cylindrical lens, which is used to focus a collimated beam into the sample. An adjustable slit adapts the numerical aperture (NA) of the illumination lens and thus the thickness of the light sheet. A second, perpendicular slit (not shown) adapts the field of view, thus making sure that no unobserved parts of the sample are illuminated. (B) The intensity distribution of a simulated light sheet is calculated for a wavelength of 488 nm and an illumination NA of 0.05 (units along both directions are in millimeters, please note the different scales). The geometry of the light sheet is adjusted to the size of the field of view, which we suggest to be twice the Rayleigh range (indicated by the two lines marked with r). The light sheet is a factor of $\sqrt{2}$ thicker and a factor of $1/\sqrt{2}$ dimmer at the edge of the field of view than in its center. This optimizes the trade-off between the thickness of the light sheet and its uniformity over the area of interest. (C) An improved setup is used to create a diffraction limited light sheet in the SPIM. The optical components and ray traces are shown in planes perpendicular (top) and parallel (bottom) to the light sheet. The adjustable gimbal-mounted mirror allows the light sheet to be aligned to the focal plane of the detection unit (not shown). Lenses L1 and L2 form a relay telescope, and the cylindrical lens and objective (obj) generate the light sheet. BFP: back focal plane.

coupled via dichroic mirrors, resulting in a multiwavelength beam. An eight channel acousto-optic tunable filter (AOTF) (AA.AOTF.8C+AAMOD.8C, Pegasus Optik GmbH, Germany) is used to select the wavelength and adjust the power. The AOTF can switch the illumination in less than 10 μs.

D. Movement unit and sample mounting

The optical arrangement is fixed. Therefore, the sample is moved along the optical axis of the detection system and through the common volume of the focal plane and the illumination plane to acquire three-dimensional stacks of images. Three computer-controlled motorized translation stages [M-111.DG, Physik Instrumente (PI) GmbH, Germany] move the sample along three dimensions and one rotary stage (M-116.DG, PI GmbH, Germany) rotates the sample around the vertical axis. This allows the acquisition of stacks of images along different directions, which is necessary for multiview image stacks. Additional degrees of freedom (nutation and declination) can be introduced to provide more flexibility when accessing more complicated samples.

The samples are embedded in a small cylinder of an agarose gel. Such biocompatible gels enable live imaging in three dimensions over periods of several days (Fig. 4). The gel consists of 0.5%–1% agarose (w/w) in a medium suitable for the specimen and the experimental conditions [e.g., phosphate-buffered saline (PBS)]. Since the sample is held in

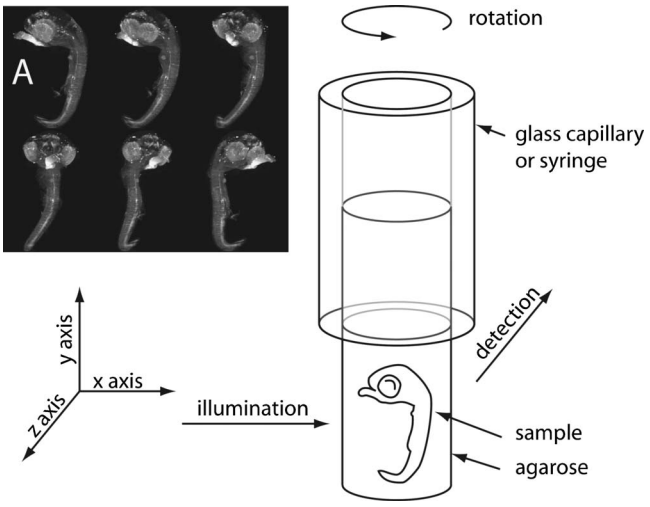

FIG. 4. Sample handling. The sample is embedded in a cylinder of a 0.5%–1% (w/w) agarose gel. A glass capillary (e.g., with an inner diameter of 1 mm) or a syringe (inner diameter of 4.7 mm) holds the agarose gel. The sample is inserted from above into an aqueous-medium-filled chamber in the SPIM. The refractive index of the agarose and the surrounding aqueous medium differs by only about 0.04%, which avoids image degradation. The capillary or syringe can be translated along three axes and rotated around its center. The rotation axis is parallel to gravity to avoid sample deformation during rotation. The latter feature allows the sample to be accessed along all sides. This is a prerequisite for multiview imaging and the reconstruction of hidden or blurred features. The insert shows the projections through stacks of images of the same sample shown in Fig. 1, but acquired along five additional directions. Each of the six views shows different details in the embryo.

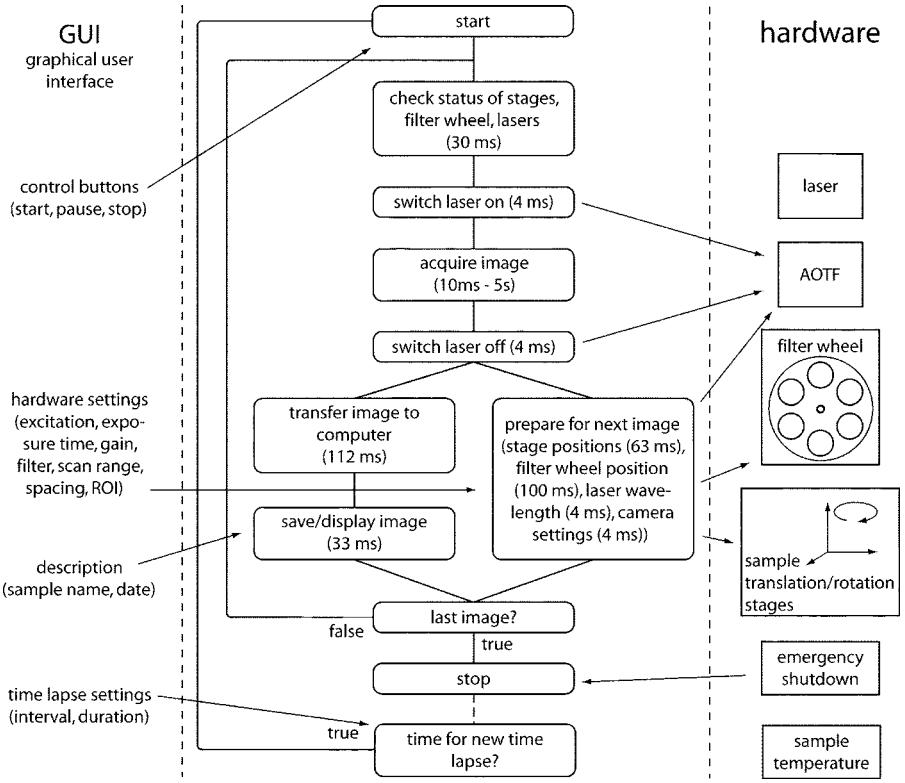

FIG. 5. Flowchart of the hardware control and image acquisition program. The kernel of SPIM's control program performs the image acquisition. It is optimized to minimize the exposure of the specimen to light. The status of the peripheral components (stages, filter wheel, and lasers) is checked prior to every sample illumination, thus making sure that everything is ready for the next image acquisition. The time needed for the image transfer from the camera to the computer and for saving the data to disk is used to set the hardware (camera settings, stage and filter positions, and the AOTF) for the next exposure. To ensure minimal exposure, the laser is switched on just prior to the image acquisition and switched off immediately after the sample has been imaged, via the AOTF. The portion of the program responsible for the acquisition of time lapses is placed external to the central loop and restarts the core routine according to time interval and duration chosen by the user.

the instrument from above, it is easily accessible from all sides. The agarose gel is not sufficiently rigid to rotate the sample without gravity causing deformations. Therefore, the particular advantage of having the rotation axis parallel to gravitation is of great importance. In the SPIM, the illumination and detection axes are horizontal, and the sample rotation axis is vertical.

Depending on the application, different chamber designs are used. With air lenses for illumination and detection, the chamber is a simple cube with four cover slips as windows. With water dipping lenses, one cover slip is replaced by a rubber sealing ring that allows the lens to be inserted into the chamber. This setup has the advantage that no additional glass surfaces are in the optical path of the detection system. This is ideal for biological samples, because the sample medium and immersion liquid are identical. In standard SPIM imaging, these chambers have a volume of about 5 ml. In addition, we build chambers for experiments where only very small amounts of solutions are available (approximately 100 μl) and others that require medium exchange under sterile conditions. Temperature control is a basic feature of all SPIM chambers and can be easily achieved with a precision in the subcentigrade range.

E. Control unit

The control unit manages the interaction between the different units during the data recording process. The kernel of the program controls the image acquisition (Fig. 5) while the timing signal is provided by the camera.

Before an image is recorded the status of the relevant mechanical parts is checked, which requires a period of 30 ms. As soon as the stages and the filter wheel have reached their target positions, the image acquisition begins. The illumination wavelength and power are set (4 ms), and following the exposure period (10 ms–5 s) the illumination is switched off via the AOTF (4 ms). The minimal exposure of the sample to light is a prime requirement, and therefore the laser is switched on only as long as images are recorded. Once the camera has captured the image, it is transferred to the computer (112 ms for a full-frame unbinned image). Saving to the hard drive and updating the display take another 33 ms. In parallel with transfer and saving, the settings for the next image are loaded; i.e., as soon as the exposure is completed, the stage and the filter wheel move to their next positions. The translation stages take 63 ms to move 1 μm, and the filter wheel takes between 80 and 300 ms to change the filter, depending on the number of positions and the load. The control loop for time lapse imaging is placed external to the central loop and restarts the recording of the next set of stacks of images following user-defined requirements. The entire image acquisition/instrument control is handled by a computer running a program written in LABVIEW (Version 7.1, National Instruments, Austin, TX).

F. Auxiliary units

The ICS in the detection unit can be used to couple in/out additional devices, e.g., a laser cutter.[13] In combination with the laser cutter, it is possible to ablate tissue in 3D and image the subsequent development in four dimensional (4D) with high spatiotemporal resolution. Such a setup will be described in a separate paper. A fluorescence lifetime imaging (FLIM) system[14] and a fluorescence recovery after photobleaching (FRAP) system are included in the setup.

TABLE II. Calculated point spread function (PSF) extents for different lenses and imaging systems. Extents are provided as a pair of numbers. The upper value is the lateral extent, and the lower the axial extent. They are determined by the full width at half maximum (FWHM) of the PSF. For mvSPIM the extent is isotropic, so only one value is given. We consider conventional (cvFM), confocal (cfFM), and two-photon (2hνFM) fluorescence microscopes, and single- and multiview SPIMs (mv). Objectives are designed for use in either air (A) or water (W). Illumination occurs at 900 nm (2hνFM) or 488 nm (all others), detection above 520 nm. The size of the field of view of the SPIM is provided in the final column, assuming a pixel pitch of 6.45 μm and 1024 $\times$1344 pixels.

Lens	cvFM	cfFM	2hνFM	SPIM	mvSPIM	FOV-SPIM
5$\times$/0.25 A	1.87 μm 40.36 μm	1.29 μm 27.88 μm	2.29 μm 49.39 μm	1.87 μm 6.00 μm	1.87 μm	1734$\times$ 1321 μm^2
10$\times$/0.3 W	1.00 μm 15.17 μm	0.69 μm 10.48 μm	1.22 μm 18.57 μm	1.00 μm 3.61 μm	1.00 μm	867$\times$ 660 μm^2
40$\times$/0.8 W	0.37 μm 1.94 μm	0.26 μm 1.34 μm	0.45 μm 2.38 μm	0.37 μm 1.34 μm	0.37 μm	217$\times$ 165 μm^2
100$\times$/1.0 W	0.29 μm 1.15 μm	0.20 μm 0.79 μm	0.36 μm 1.40 μm	0.29 μm 0.82 μm	0.29 μm	86.7$\times$ 66.0 μm^2

III. PERFORMANCE

The resolution of the SPIM is defined by the properties of the detection and the illumination setup. The lateral resolution is determined by the detection objective lens and is therefore the same as in a regular fluorescence wide-field microscope. The axial resolution is dominated by the thickness of the light sheet and is less affected by the PSF defined by the NA of the detection lens. The situation is thus different than in epifluorescence setups. Therefore, contrary to other microscopes, the isotropy of the PSF is much better for low NA systems. It should be noted that particularly for low-magnification systems, the axial resolution of the SPIM is far superior compared to other types of microscopes. But even for high NA systems the imaged volumes are in the same range for SPIM and confocal microscopes.

Table II lists the calculated resolutions of various fluorescence imaging systems that could be considered suitable for the type of samples for which SPIM is designed (i.e., 50 μm–5 mm in size). Calculations were done as described in Ref. 10.

IV. DISCUSSIONS

Single plane illumination fluorescence microscopy is a technique that uses a thin light sheet for the illumination of the focal plane of the detection objective lens. It provides optical sectioning and illuminates only those fluorophores that are in focus. The system combines the advantages of wide-field methods (speed, flexibility, and dynamic range) with those of a confocal arrangement (optical sectioning). SPIM provides quantitative three-dimensional maps of the distribution of a fluorophore, for example, the expression pattern of GFP-labeled protein, with high spatiotemporal resolution[15] and an excellent signal to noise ratio. Since SPIM uses the fluorophores much more efficiently than a comparable confocal or conventional microscope, SPIM induces much less bleaching. This enables imaging with a higher temporal resolution or over a longer period of time [see online supplement S1 (Ref. 16)]. The mounting of the sample, e.g., in agarose gels and an aqueous solution, allows the imaging of live samples under sample-friendly conditions.

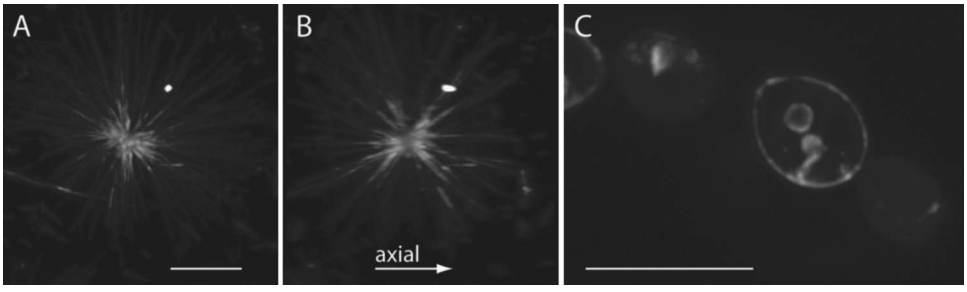

FIG. 6. Examples of images recorded with high numerical aperture. [(A) and (B)] The maximum-intensity projections of a three-dimensional stack of a tubulin-Alexa-488-labeled aster after it formed in BRB80 buffer. (A) The projection along the detection axis illustrates the diffraction limited resolution of the objective lens in the lateral direction. No background is visible, because out-of-focus fluorophores are not excited. Scale bar 10 μm. (B) The projection along the illumination axis demonstrates the axial resolution of the system. The detection axis is horizontal in this image. Scale as in A. (C) Maximum-value projection of a part of a stack showing Ady2-GFP-labeled yeast cells. This is one frame out of a time lapse (movie included as online supplement S1) with 191 time points. This long movie is possible because of the reduced photobleaching in the SPIM, when compared to other sectioning microscopic techniques. λ_{ill}=488 nm, detection filter Chroma HQ 500 LP, detection lens Carl Zeiss Achroplan 100$\times$/1.0 W, scale bar 10 μm. Microtubule aster prepared by Francesco Pampaloni and yeast sample prepared by Christof Taxis.

The volumes imaged with SPIM, which determine the maximum size of the sample that can be imaged, are of the same order as those that can be achieved with a confocal microscope with medium-to-high NA objectives. With the low NA lenses appropriate for millimeter-sized samples, SPIM gives a substantial improvement over a confocal microscope.

For some experiments in life science the *in vivo* conditions and the good depth penetration are essential. In online supplement S2,[16] we present as an example a time lapse of muscle development (myoblast fusion) of a *drosophila melanogaster* embryo. The stacks in Fig. 1 and the movie in the online material S2 show the good depth penetration of rather big samples. This is due to the relatively low NA of the illumination system. Figure 6 shows two examples for high resolution applications of the SPIM. (A) and (B) show a microtubule aster in the lateral and lateral-axial views, demonstrating the good isotropy of the resolution [a movie of maximum projections of the stack under increasing angles is shown as an online supplement S3 (Ref. 16)].

ACKNOWLEDGMENTS

The authors wish to thank the EMBL workshop engineers Alfons Riedinger, Georg Ritter, Wolfgang Dilling, and Leo Burger for their contributions. We also thank Sebastian Enders for his contributions to EMBL's first SPIM. The biological samples were provided by Christof Taxis (yeast samples), Francesco Pampaloni (asters), Marina Ramialison and Jochen Wittbrodt (medaka), and Paulo Cunha and Eileen Furlong (drosophila). Uros Krzic and Sonja Welsch critically read the manuscript.

[1] M. Chalfie, Y. Tu, G. Euskirchen, W. W. Ward, and D. C. Prasher, Science **263**, 802 (1994).
[2] R. Helm, A. B. Cubitt, and R. Y. Tsien, Nature (London) **373**, 663 (1995).
[3] A. H. Voie, D. H. Burns, and F. A. Spelman, J. Microsc. **170**, 229 (1993).
[4] E. Fuchs, J. S. Jaffe, R. A. Long, and F. Azam, Opt. Express **10**, 145 (2002).
[5] J. Huisken, J. Swoger, F. Del Bene, J. Wittbrodt, and E. H. K. Stelzer, Science **305**, 1007 (2004).
[6] J. B. Pawley, *Handbook of Biological Confocal Microscopy*, 3rd ed. (Plenum, New York, 2006).
[7] S. Lindek, J. Swoger, and E. H. K. Stelzer, J. Mod. Opt. **46**, 843 (1999).
[8] E. H. K. Stelzer, S. Lindek, S. Albrecht, R. Pick, G. Ritter, N. J. Salmon, and R. Stricker, J. Microsc. **179**, 1 (1995).
[9] E. H. K. Stelzer and S. Lindek, Opt. Commun. **111**, 536 (1994).
[10] C. J. Engelbrecht and E. H. Stelzer, Opt. Lett. **31**, 1477 (2006).
[11] P. J. Keller, F. Pampaloni, and E. H. K. Stelzer, Curr. Opin. Cell Biol. **18**, 117 (2006).
[12] P. J. Verveer, J. Swoger, F. Pampaloni, K. Greger, and E. H. K. Stelzer, Nat. Methods (accepted for publication).
[13] J. Colombelli, S. W. Grill, and E. H. K. Stelzer, Rev. Sci. Instrum. **75**, 472 (2004).
[14] K. Greger, P. Bastiaens, and E. H. K. Stelzer, *Abstract Book Focus on Microscopy* (Jena, 2005), p. 225.
[15] C. Taxis, C. Maeder, S. Reber, N. Rathfelder, K. Greger, K. Miura, E. H. K. Stelzer, and M. Knop, Traffic (Oxford, U. K.) **7**, 1628 (2006).
[16] See EPAPS Document No. E-RSINAK-78-230701 for movies of 1)comparison of the bleaching in SPIM and DeltaVision, 2) the drosophila muscle development and 3) rotating maximum projections of a microtubule aster. These documents can be reached via a direct link in the online article's HTML reference section or via the EPAPS homepage (http://www.aip.org/pubservs/epaps.html).
[17] http://ani.embl.de:8080/mepd/MdbShowClone01?cloneID=8299